IEEE Access
Multidisciplinary ⋮ Rapid Review ⋮ Open Access Journal

Received May 19, 2020, accepted June 8, 2020, date of publication June 11, 2020, date of current version June 24, 2020.

Digital Object Identifier 10.1109/ACCESS.2020.3001587

Nearest-Level Control Method With Improved Output Quality for Modular Multilevel Converters

MINH HOANG NGUYEN AND SANGSHIN KWAK, (Member, IEEE)
School of Electrical and Electronics Engineering, Chung-Ang University, Seoul 06974, South Korea

Corresponding author: Sangshin Kwak (sskwak@cau.ac.kr)

This work was supported by the National Research Foundation of Korea (NRF), funded by the Korean Government (MSIT), under Grant 2020R1A2C1013413.

ABSTRACT Nearest-level control (NLC) is a popular technique used in modular multilevel converters (MMCs) with a large number of submodules (SMs) owing to the NLC's flexibility and ease of implementation. However, in medium-voltage applications, MMCs contain a relatively low number of SMs, and the drawbacks of the NLC methods emerge, wherein the poor quality of output voltages and currents result in high total harmonic distortion, large ripples in SM capacitor voltages, and unsuppressed circulating currents. Several NLC methods have been proposed to handle these problems, but they do not satisfy all the control objectives simultaneously. This paper proposed a modified NLC capable of enhancing the output quality of MMCs with low number of SMs without deteriorating the control objectives. Unlike previously reported NLC methods, instead of directly calculating the numbers of SMs from the upper and lower arm voltage references, the difference and total number of SMs are obtained from the output voltage reference and circulating current control, respectively. Hence, the numbers of SMs in the upper and lower arms are acquired by simply solving a system of first-order two-variable equations. The simulated and experimental results for a single-phase MMC system were used to verify the appropriateness and effectiveness of the proposed modified NLC method.

INDEX TERMS Nearest-level control, modular multilevel converter, increase level number, output voltage quality, circulating current.

I. INTRODUCTION

Multilevel converters have gained wider acceptance over two-level converters owing to their improved waveform qualities, reduced semiconductor losses, low electromagnetic interferences (EMIs), and common-mode voltages (CMV). The most general topologies available for multilevel converters are neutral-point-clamped (NPC) converters, flying capacitor (FC) converters, cascaded H-bridge (CHB) converters, and modular multilevel converters (MMCs) [1]–[5]. The MMC has a few additional attractive features, such as modular design, scalability, and lower losses, compared to the other multilevel converters. Since the invention of the MMC by Marquardt in 2003 [6], it has been analyzed extensively for medium-to-high-power applications. Although the MMC has an attractive topology with various prominent features, it requires a complicated control strategy for optimal operation. In addition to the output current and voltage control found in other multilevel converter topologies, submodule (SM) capacitor voltages and circulating currents should be regulated simultaneously [7]–[9]. An appropriate control strategy is therefore crucial for an MMC because of the impact on output harmonics, filter size, switching frequency, power losses, etc. Similar to other power converter topologies, pulse-width modulation (PWM) with different configurations that include phase- and level-shifted carriers is the most common realization for MMCs [10]–[13]. The PWM control schemes offer low total harmonic distortion (THD), but these methods share some common drawbacks such as high switching frequency and complicated placement of a large number of SMs. Unlike PWM methods, the nearest-level control (NLC) methods [14], [15] eliminate the use of

The associate editor coordinating the review of this manuscript and approving it for publication was Meng Huang.

the triangular carrier wave, thereby allowing a lower switching frequency and simpler implementation. However, the conventional NLC method is especially suitable for an MMC with a relatively large number of SMs because this NLC scheme ensures adequate output quality. For MMCs with lower number of SMs, as are commonly used in medium-voltage applications, the use of the conventional NLC method results in poorer quality waveforms than PWM strategies. In addition, as a direct modulation, the conventional NLC method does not include control of the circulating currents, thus resulting in a high root-mean-squared (rms) value of the circulating currents and a large SM capacitor voltage ripple.

To enhance the quality of the output waveforms, especially the output voltage, a level-increased and improved level-increased NLC methods were proposed in [16] and [17], respectively, to increase the number of output voltage levels to $2N + 1$ and to reduce the THD of the output voltages. Unlike the conventional NLC method, the level-increased NLC methods can modify the references of the upper and lower arm voltages by inserting small offsets, which result in changes to the alignments of the transition edges between the upper and lower arm voltages. In [16], the level-increased NLC I (2015) varied the total number of inserted SMs between N and $N + 1$. This resulted in changes in the average voltages of SM capacitors and consequently amplitude changes of the output voltage. The improved level-increased NLC II (2016) method in [17] solved the aforementioned problem by changing the small offset between the positive and negative value alternately at double fundamental frequency. This resulted in the average number of inserted SMs being maintained at N rather than varying among N, $N-1$, and $N+1$. In addition, the average voltages of the SM capacitors remained unchanged. Although the output voltage waveform was improved with the level-increased NLC I, this control scheme did not suppress the circulating current, whereas the level-increased NLC II adjusted the initial phase of the small offset to control the SM capacitor voltage ripple and the circulating current. However, the change in the initial phase was dependent on the power factor angle and could impact to output quality. The NLC method with circulating current control (NLC-C) in [18] replaced the small offset by a small second-order harmonic control term. For the NLC-C method, the maximum number of output voltage levels was not less than $2N - 1$ and could possibly be $2N + 1$. Compared to the two level-increased NLC methods, the circulating current with the NLC-C scheme was minimized by eliminating the second-order harmonic, but the effectiveness of the NLC-C was dependent on the sampling frequency and the inserted term. The predictive NLC proposed in [19] regulated the output current and circulating current using associated predictive references based on deadbeat control. The output current and circulating current under the predictive NLC method were controlled well but resulted in high switching frequency and high THD output voltage. Additionally, the predictive NLC method required an accurate mathematical model of the MMC, which is sensitive to parameter mismatches. In [20], the number of inserted SMs in the upper and lower arms of the conventional NLC method were adjusted to control the circulating current using a limit controller. The limit controller allowed the peak-to-peak value of the circulating current to be significantly reduced compared to the conventional NLC method, but the adjustment of the number of inserted SMs in the upper and lower arms with this method could not be controlled. This might result in deterioration of the output voltage quality. Recently, an NLC method with circulating harmonic current suppression with deadbeat control was proposed in [21], where the numbers of inserted SMs in the upper and lower arms from the level-increased NLC II were adjusted based on the deadbeat controller to regulate the circulating current. This control scheme inherited the merits of both the level-increased NLC II and deadbeat controller to improve the output quality and control the circulating current.

This paper proposes a modified NLC method to improve the output quality of the MMC with a low number of SMs and to solve the problems observed in previous NLC methods. Unlike the previous NLC methods, the proposed technique uses the output voltage reference to calculate the difference in the number of inserted SMs in the lower and upper arms, as this difference defines the first condition regarding output voltage control. The first predefined condition guarantees accuracy of the output voltage level number and smooth transition among the adjacent output voltage levels. The circulating current control is implemented by selecting the total number of inserted SMs via a simple comparison between the measured circulating current and reference value. The total number of inserted SMs defines the condition for the circulating current control. By combining two predefined conditions, the numbers of inserted SMs in the upper and lower arms can be calculated by solving a system of first-order two-variable equations. The proposed method guarantees the control objectives of the MMC and improves the output quality with a low THD output current and voltage while suppressing the circulating current compared to previous NLC methods. The proposed method's performance was confirmed via simulations and experiments.

The rest of the paper is structured as follows. Section II discusses the topology and mathematical model for a single-phase MMC. Section III provides an overview of the conventional NLC method and any relevant NLC methods proposed in existing studies. Section IV introduces the proposed modified NLC technique. The simulated and experimental results for the proposed control scheme are given in Section V, and the concluding remarks are presented in Section VI.

II. MATHEMATICAL MODEL AND OPERATION OF THE MMC

The circuit configuration of the three-phase MMC is shown in Fig. 1(a). Each phase leg of the MMC contains two arms with N identical series-connected half-bridge SMs per arm.

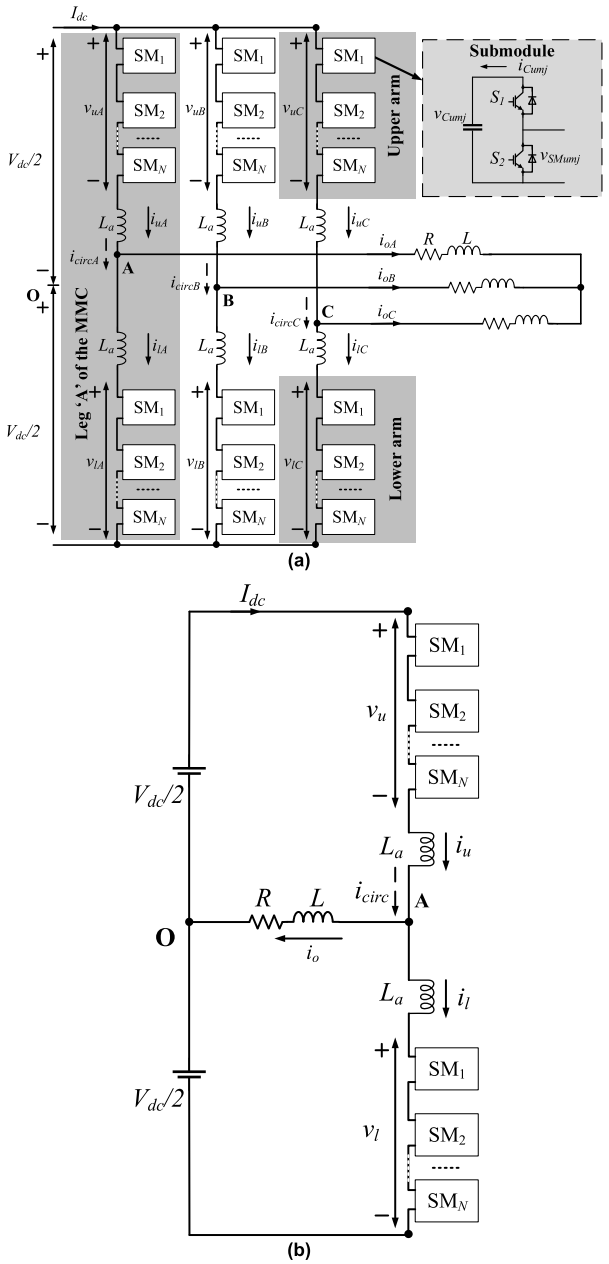

FIGURE 1. Circuit configuration of the MMC: (a) three-phase MMC and half-bridge SM; (b) single-phase MMC.

In each arm, an inductor L_a is connected in series with the SMs. Owing to the symmetry of the three-phase MMC, the analysis was carried out for each phase leg, as shown in Fig. 1(b). The upper and lower arm voltages are denoted by v_u and v_l, respectively, whereas the upper and lower arm currents and output current are i_u, i_l, and i_o, respectively. Applying the Kirchhoff's current law to the single-phase MMC circuit, the output current can be expressed as

$$i_o = i_u - i_l. \tag{1}$$

The mean value of the upper and lower arm currents is referred to as the circulating current and is expressed as follows:

$$i_{circ} = \frac{i_u + i_l}{2}. \tag{2}$$

Applying Kirchhoff's voltage law, as shown in Fig. 1(b), the voltage relationship can be defined as

$$\frac{V_{dc}}{2} - v_u - L_a\frac{di_u(t)}{dt} - Ri_o - L\frac{di_o(t)}{dt} = 0, \tag{3}$$

$$-\frac{V_{dc}}{2} + v_l + L_a\frac{di_l(t)}{dt} - Ri_o - L\frac{di_o(t)}{dt} = 0. \tag{4}$$

Adding (3) and (4) and using i_o from (1), the output voltage is expressed by

$$v_o = Ri_o + L\frac{di_o(t)}{dt} = \frac{v_l - v_u}{2} - \frac{L_a}{2}\frac{di_o(t)}{dt}. \tag{5}$$

The upper and lower arm voltages of the single-phase MMC can also be described by

$$v_u = N_u v_{Cu\_avg}, \tag{6}$$

$$v_l = N_l v_{Cl\_avg} \tag{7}$$

where N_u and N_l are the numbers of inserted SMs in the upper and lower arms, respectively. v_{Cu_avg} and v_{Cl_avg} are the average capacitor voltages in the associated arms. Assuming that the SM capacitor voltages are maintained steadily at a nominal value $V_C^* = V_{dc}/N$ and the voltage drops on the arm inductors L_a are negligible, the output voltage can be expressed as

$$v_o = \frac{N_l - N_u}{2}V_C^*. \tag{8}$$

III. NLCs IN MMCs

Fig. 2(a) depicts the control diagram for the conventional NLC method. The upper and lower arm voltage references are first normalized by the nominal value of the SM capacitor voltage V_C^*; then, the round function generates an integral number of inserted SMs corresponding to the nearest voltage level. The acquired number for the SMs is then sent to the voltage sorting algorithm, which generates the switching signals to operate the MMC. The numbers of inserted SMs in the upper and lower arms are calculated by

$$N_{u\_final}^* = round\left(N\frac{v_u^*}{V_C^*}\right), \tag{9}$$

$$N_{l\_final}^* = round\left(N\frac{v_l^*}{V_C^*}\right), \tag{10}$$

where

$$v_u^* = \frac{V_{dc}}{2}\left[1 - Mcos\left(2\pi f_o t\right)\right], \tag{11}$$

$$v_l^* = \frac{V_{dc}}{2}\left[1 + Mcos\left(2\pi f_o t\right)\right]. \tag{12}$$

Fig. 3(a) illustrates the voltage waveforms of the conventional NLC method with $N = 7$ and modulation index $M = 1$ for a fundamental period of T_o. The resulting output voltage v_o^{round} can be observed to have a maximum level number of $N + 1$ with a step height of V_C^* and a maximum possible error

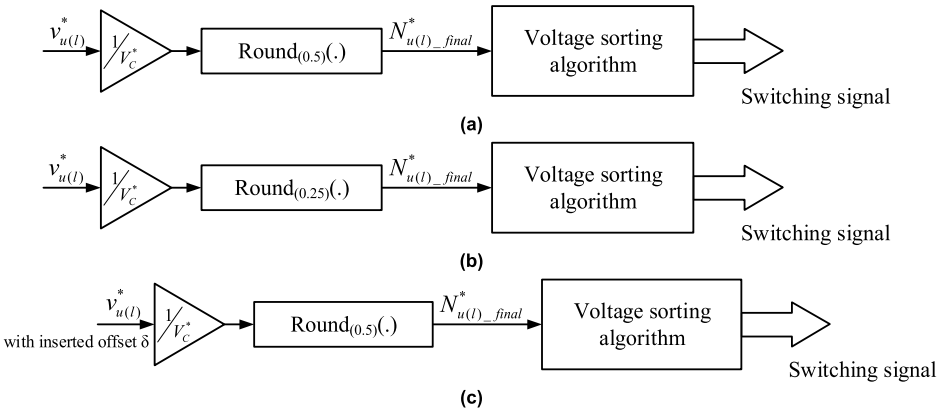

FIGURE 2. Control diagram representing a (a) conventional NLC [15], (b) level-increased NLC I [16], and (c) level-increased NLC II [17].

of $0.5V_C^*$. The waveforms of the upper and lower arm step voltages v_u^{round} and v_l^{round} are symmetrical to each other and to the vertical $y = V_{dc}/2$ line. Therefore, all the transition instants of v_u^{round} and v_l^{round} are aligned (two such pairs are shown by black lines in Fig. 3(a)).

Although implementing the conventional NLC is straightforward, the MMC system is recommended to contain a large number of SMs so that the output quality is adequate compared to the conventional NLC. Hence, two level-increased NLC methods were developed in 2015 and 2016, especially for MMC systems with lower numbers of SMs, to improve the output quality. The working principles of the two level-increased NLC methods are illustrated in Fig. 2(b) and 2(c), respectively. As for the level-increased NLC I, by replacing the standard round function with an altered round function $round_{0.25}$ (.), the control scheme shifts the instants of step changes in the upper and lower arm voltages. Then, the numbers of inserted SMs in the upper and lower arms are calculated by

$$N^*_{u\_final} = round_{0.25}\left(N\frac{v^*_u}{V^*_C}\right), \tag{13}$$

$$N^*_{l\_final} = round_{0.25}\left(N\frac{v^*_l}{V^*_C}\right). \tag{14}$$

The modified round function $round_{0.25}$ (.) is equivalent to adding an offset term $\delta = 0.25$ to the round function as $round_{0.5}\,(x + 0.25)$, which then produces

$$N^*_{u\_final} = round\left(N\frac{v^*_u}{V^*_C} + 0.25\right), \tag{15}$$

$$N^*_{l\_final} = round\left(N\frac{v^*_l}{V^*_C} + 0.25\right). \tag{16}$$

The level-increased NLC I method can be understood as adding offsets to the upper and lower arm voltage references and breaking the vertical symmetry of the resulting step voltage v_u^{round} and v_l^{round} so that all the transition instants are unaligned, as shown in Fig. 3(b). Using the modified round function $round_{0.25}$ (.), the MMC output voltage has $2N + 1$ levels with a step height that is reduced to $0.5V_C^*$. The output voltage quality is therefore improved compared with that of the conventional NLC method. However, this technique causes changes to the average voltages of the SM capacitors and consequently results in amplitude changes in the output voltage.

The level-increased NLC II method shown in Fig. 2(c) resolves the problems of both the conventional NLC and level-increased NLC I methods by inserting an offset term δ in the round function and also alternating the offset term δ between the positive and negative values at the double fundamental frequency. By applying this NLC control scheme, the numbers of inserted SMs in the upper and lower arms are calculated as

$$N^*_{u\_final} = round\left(N\frac{v^*_u}{V^*_C} + \delta\right), \tag{17}$$

$$N^*_{l\_final} = round\left(N\frac{v^*_l}{V^*_C} + \delta\right). \tag{18}$$

The offset term δ can be varied from -0.5 to 0.5. The change of the offset term δ at the double fundamental frequency results in variation of the total number of inserted SMs as N, $N - 1$, or $N + 1$, as shown in Fig. 4(c). Additionally, the total number of inserted SMs with the conventional NLC method can be considered $\delta = 0$, as shown in Fig. 4(a), whereas the total number of inserted SMs with the level-increased NLC I is similar to $\delta = 0.25$, as in Fig. 4(b). From Fig.4 (b), the total number of inserted SMs with the level-increased NLC I can be seen to vary between N and $N+1$. Hence, the average SM capacitor voltages are changed. Meanwhile, the level-increased NLC II maintains the average number of inserted SMs at N to stabilize the average SM capacitor voltage at the nominal value V_C^*.

The output voltages from the two level-increased NLC control schemes are improved compared to that of the conventional NLC. However, another control objective of the MMC is suppression of the circulating current, which is not guaranteed. In [18], a small second-order harmonic control term was inserted at the upper and lower arm voltage references.

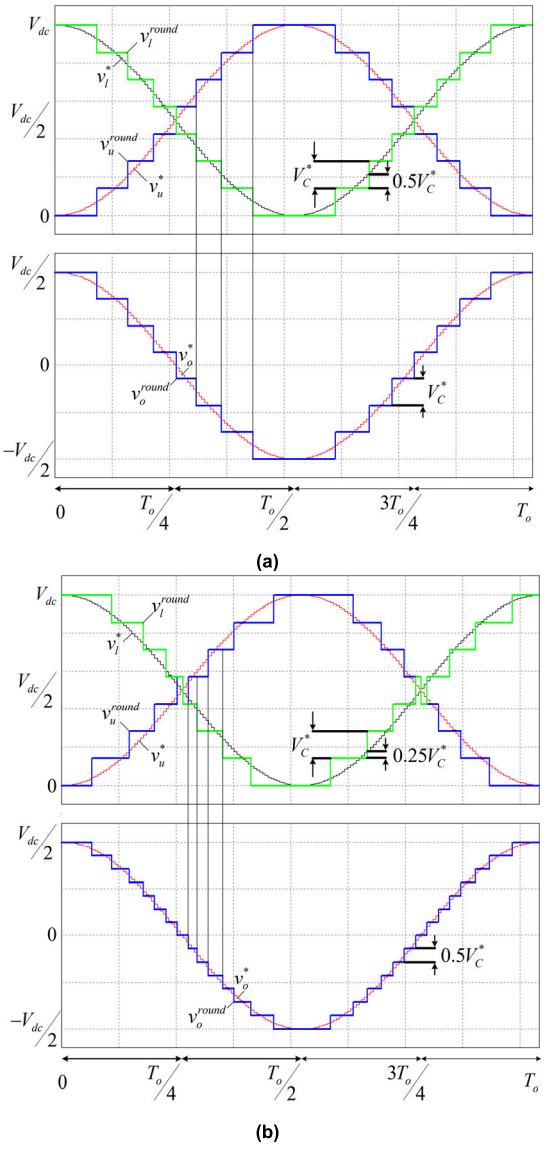

FIGURE 3. Working principles of the (a) conventional NLC and (b) level-increased NLC.

These voltage references considering the circulating current control can be expressed as

$$v_u^* = \frac{V_{dc}}{2}\left[1 - Mcos\left(2\pi f_o t\right) - m_2\right], \tag{19}$$

$$v_l^* = \frac{V_{dc}}{2}\left[1 + Mcos\left(2\pi f_o t\right) - m_2\right] \tag{20}$$

where m_2 is the inserted circulating current control term that is calculated as

$$m_2 = M_2 cos\left(4\pi f_o t\right). \tag{21}$$

The detailed calculation of m_2 from the NLC-C scheme can be found in [18]. The control diagram of the NLC-C is depicted in Fig. 5(a). Although the term m_2 can help suppress the second-order harmonic component in the circulating current, the effectiveness of such circulating current control is dependent on the energy storage coefficient k_E [22], which represents the minimum energy storage required to transfer the rated VA volume of the converter.

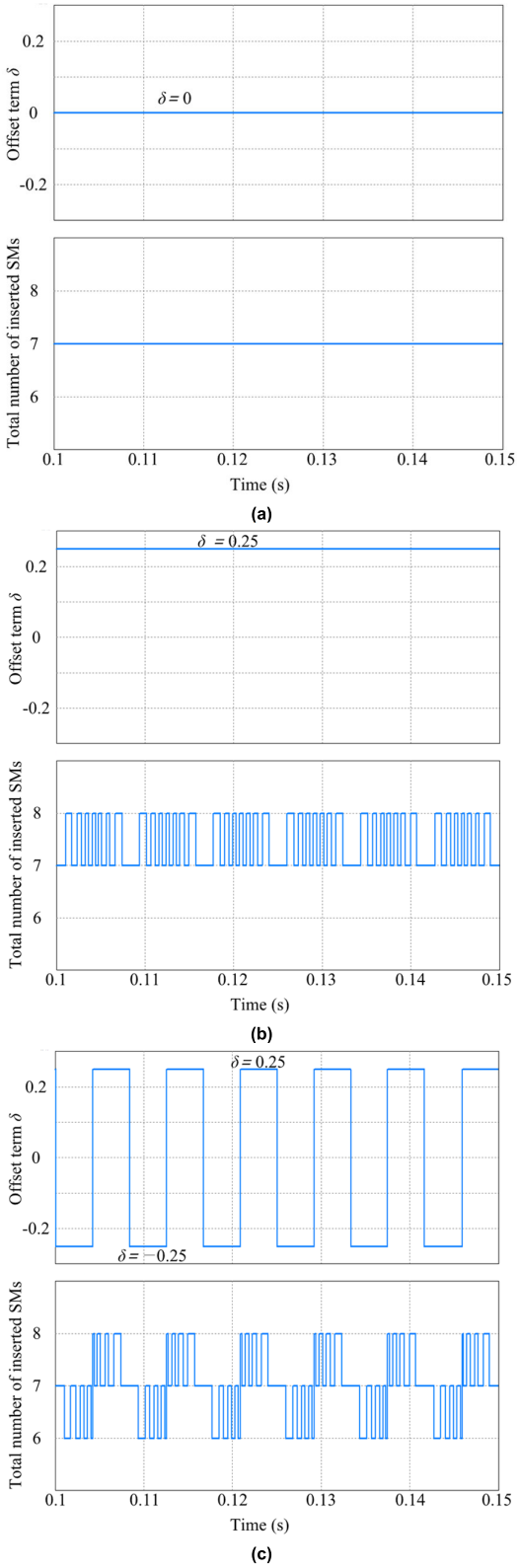

FIGURE 4. Total numbers of inserted SMs when (a) $\delta = 0$, (b) $\delta = 0.25$, and (c) δ alternating at double fundamental frequency.

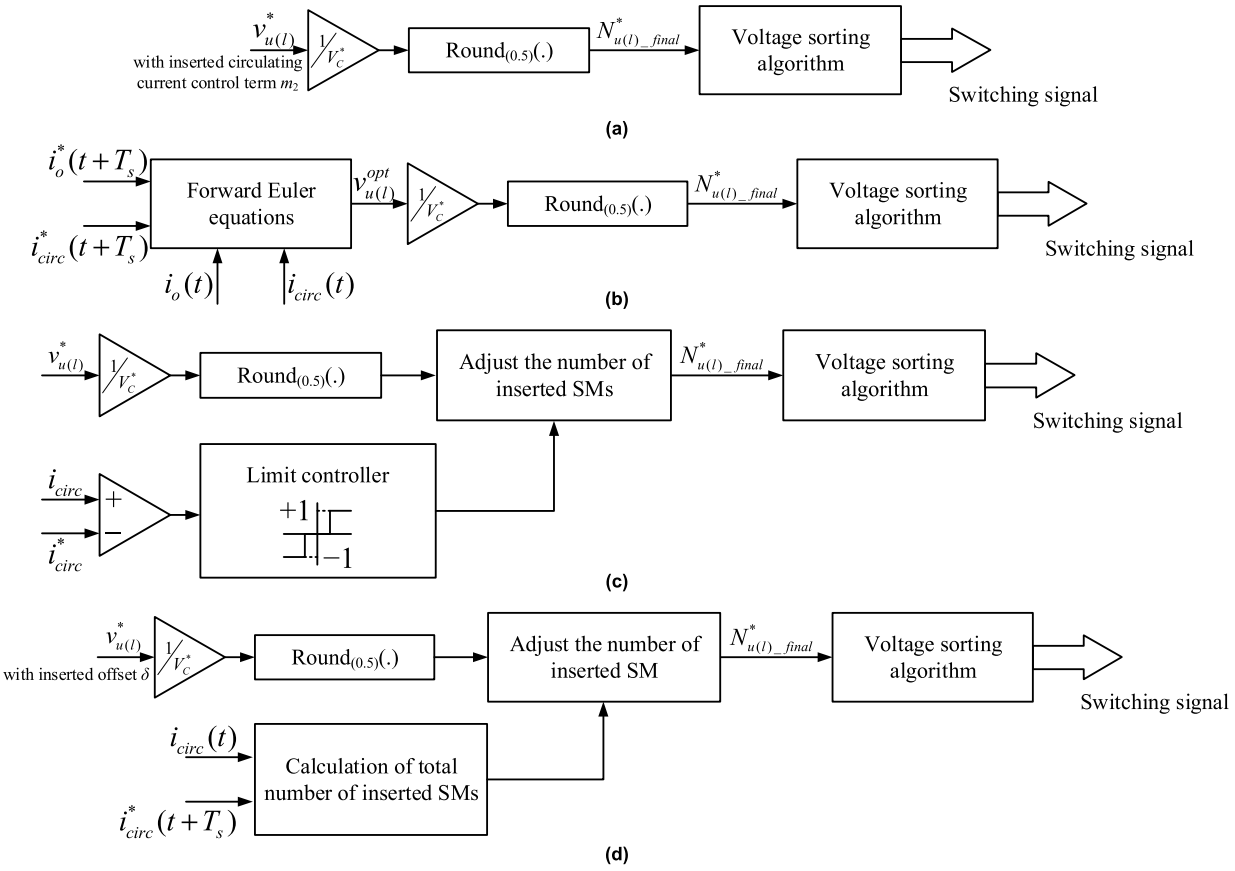

FIGURE 5. Control diagrams of the (a) NLC-C [18], (b) predictive NLC [19], (c) NLC with modified circulating current control [20], and (d) level-increased NLC with deadbeat control [21].

In [19], the authors proposed a control scheme named predictive NLC, which inherits the advantages of both predictive control and NLC, as shown in Fig. 5(b). The general idea of the predictive NLC is to use the predicted values of the output and circulating currents to generate the optimal upper and lower arm voltage references. Using the Euler approximation [23], the discrete-time model of the output and circulating currents can be obtained from (3) and (4), respectively, as

$$i_o\left(t+T_s\right)=\left(\frac{T_s}{2L+L_a}\right)\left[v_l\left(t\right)-v_u(t)\right]+\left(1-\frac{2RT_s}{2L+L_a}\right)i_o\left(t\right), \tag{22}$$

$$i_{circ}\left(t+T_s\right)=\left(\frac{T_s}{2L_a}\right)\left[V_{dc}-v_l\left(t\right)-v_u(t)\right]+i_{circ}\left(t\right). \tag{23}$$

The optimal value of the upper and lower arm voltages can be obtained from (22) and (23) by replacing $i_o\left(t+T_s\right)$ and $i_{circ}\left(t+T_s\right)$ with their respective reference values $i_o^*(t+T_s)$ and $i_{circ}^*(t+T_s)$. Hence, the optimal upper and lower arm voltages are given as

$$v_u^{opt}=\frac{V_{dc}}{2}-\frac{A+B}{2}, \tag{24}$$

$$v_l^{opt}=\frac{V_{dc}}{2}+\frac{A-B}{2}, \tag{25}$$

where

$$A=\frac{2L+L_a}{T_s}\left[i_o^*\left(t+T_s\right)-i_o\left(t\right)\right]+2Ri_o\left(t\right), \tag{26}$$

$$B=\frac{2L}{T_s}\left[i_{circ}^*(t+T_s)-i_{circ}(t)\right]. \tag{27}$$

The predictive NLC is based on the deadbeat controller used to regulate the output and circulating currents. However, the output performance of this NLC technique is strongly dependent on the mathematical model of the MMC system. The predictive NLC is sensitive to parameter mismatches and has a high switching frequency.

The NLC method with modified circulating current control depicted in Fig. 5(c) combines the conventional NLC method and a limit controller to regulate the MMC system. By adjusting the numbers of inserted SMs in the upper and lower arms from the conventional NLC method based on the difference between the measured and reference circulating currents i_{circ} and i_{circ}^*, respectively, this control scheme regulates the circulating current by limiting the peak-to-peak value within a

fixed band. However, adjusting the number of inserted SMs of the conventional NLC method without considering the output voltage level might lead to degradation of the output voltage waveforms.

Recently, the level-increased NLC with deadbeat control has been combined with the level-increased NLC II and deadbeat control to regulate the MMC system, as shown in Fig. 5(d). The total number of inserted SMs is acquired using deadbeat control for the circulating current. First, the total voltage of the upper and lower arms is obtained from the discrete-time model of the circulating current (23) and by replacing $i_{circ}(t+T_s)$ with $i^*_{circ}(t+T_s)$, as in the predictive NLC method, which can be expressed as:

$$\begin{aligned} V^*_{\Sigma} &= v_u(t) + v_l(t) \\ &= V_{dc} - \frac{2L_a}{T_s}\left[i^*_{circ}(t+T_s) - i_{circ}(t)\right]. \end{aligned} \tag{28}$$

Accordingly, the total number of inserted SMs, considering the circulating current control, is deduced as

$$N^*_{\Sigma 2} = \text{int}\left[N\frac{V^*_{\Sigma}}{V_{dc}}\right]. \tag{29}$$

Hence, the obtained numbers of inserted SMs in the upper and lower arms from the level-increased NLC II part are adjusted based on the total number of inserted SMs by considering the circulating current control and predefined conditions.

IV. PROPOSED NLC

A. OUTPUT VOLTAGE CONTROL

The basic idea behind the NLC method is to use the upper and lower arm voltage references to generate the number of inserted SMs in the corresponding arm. However, adjustment of these numbers of inserted SMs in the upper and lower arms to guarantee the control objective might deteriorate the output voltage quality or the average SM capacitor voltages [17]. To resolve this problem, the proposed modified NLC uses the output voltage and circulating current references to calculate the numbers of inserted SMs in the upper and lower arms. The proposed method also guarantees the control objectives of the MMC and improves the output quality compared to previous NLC methods.

The control diagram depicting the proposed technique is illustrated in Fig. 6. For output voltage control, the output voltage reference can be defined as

$$v^*_o = \frac{V_{dc}}{2}cos(2\pi f_o t). \tag{30}$$

From (8), the output voltage under ideal conditions is calculated by multiplying the difference in the numbers of inserted SMs in the upper and lower arms, N_{diff}, with the nominal SM capacitor voltage value V^*_C. From (8) and (30), the normalized output voltage can be given as

$$v_{o\_nom} = \frac{N_{diff}}{2} = \frac{N_l - N_u}{2} = round\left(N\frac{v^*_o}{V^*_C}\right). \tag{31}$$

For the $2N+1$ output voltage level, the differences in the numbers of inserted SMs in the upper and lower arms vary among $-N, -N+1 \ldots, 0 \ldots, N-1, N$ depending upon the associated output voltage level. The output voltage level is described as

$$l = N_l - N_u + N + 1. \tag{32}$$

With different combinations of $N_l - N_u$, the resulting output voltage levels range from 1 to $2N+1$ whereas the output voltage correspondingly ranges from $-V_{dc}/2$ to $V_{dc}/2$. The relationship between the output voltage and numbers of inserted SMs in the upper and lower arms are shown in Table 1.

TABLE 1. Correlation between the differences in the numbers of inserted SMs and output voltages.

Difference in the no. of inserted SMs N_{diff}	Output voltage level l	Output voltage
$-N$	1	$-V_{dc}/2$
$-N$+1	2	$-V_{dc}/2 + V^*_C/2$
$-N$+2	3	$-V_{dc}/2 + V^*_C$
…	…	…
0	N+1	0
…	…	…
N–2	2N–1	$V_{dc}/2 - V^*_C$
N–1	2N	$V_{dc}/2 - V^*_C/2$
N	2N+1	$V_{dc}/2$

By applying the output voltage reference and the round function, the difference between the numbers of inserted SMs in the upper and lower arms is generated. These inserted SMs in the two arms are not directly calculated during this step, but the output voltages and the transitions among the closest output voltage levels are guaranteed, which improves the output quality of the MMC system.

B. CIRCULATING CURRENT CONTROL

To regulate the circulating current without deteriorating the quality of the output voltage and output current as well as the average SM capacitor voltage, the numbers of inserted SMs in the upper and lower arms should be calculated correctly. Using (6), (7), and (23), the discrete-time model of the circulating current can be expressed as

$$i_{circ}(t+T_s) = \left(\frac{T_s}{2L_a}\right)\left[NV^*_C - (N_u+N_l)V^*_C\right] + i_{circ}(t). \tag{33}$$

In the ideal condition, if the total number of inserted SMs in the upper and lower arms N_{sum} equals N, the circulating current will remain unchanged over time. However, in the $2N+1$ output voltage level MMC system, the total number

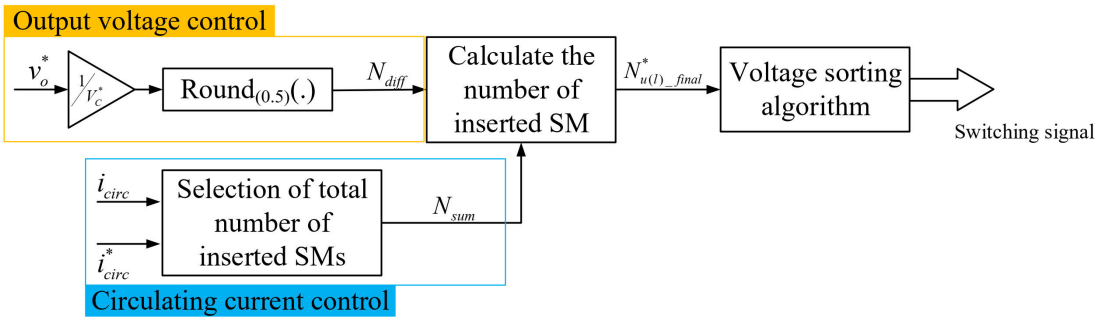

FIGURE 6. Control diagram depicting the proposed NLC.

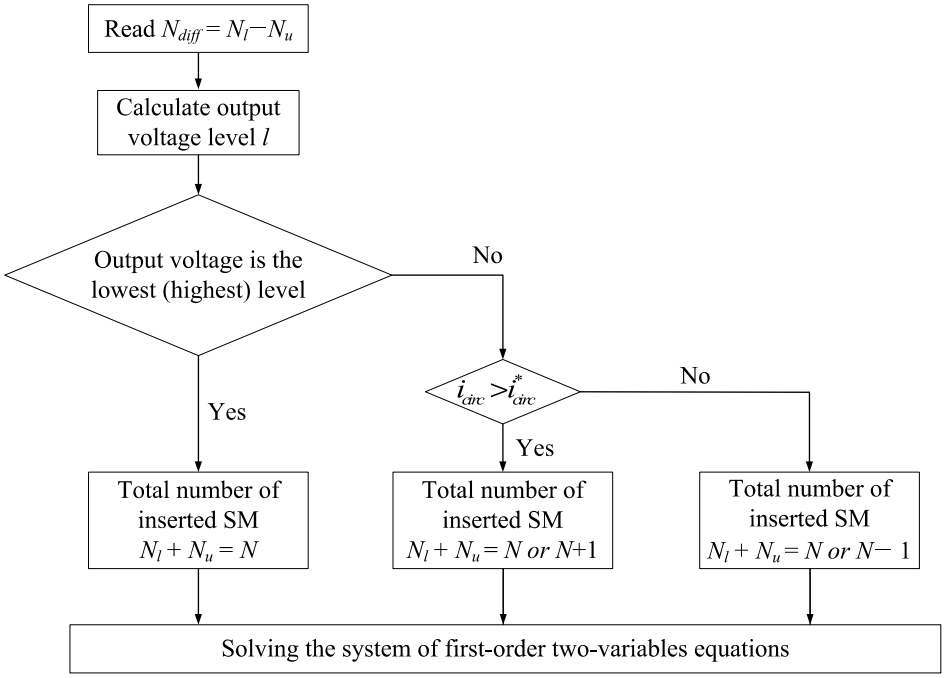

FIGURE 7. Diagram representing calculation of the number of inserted SMs in the upper and lower arms.

of inserted SMs in the upper and lower arms can be N, $N-1$, or $N+1$ [24]. This means that with the varying number of inserted SMs in the upper and lower arms, the circulating current in the next sampling instant can increase, decrease, or remain unchanged. When the total number of inserted SMs in the upper and lower arms equals $N-1$, (33) can be expressed as

$$i_{circ}(t+T_s) = \left(\frac{T_s}{2L_a}\right)\left[NV_C^* - (N-1)V_C^*\right] + i_{circ}(t). \quad (34)$$

In this case, the first term of (34) will be positive, and the circulating current difference tends to increase according to

$$\Delta i_{circ} = \frac{T_s}{2L_a} V_C^*. \quad (35)$$

However, if the total number of inserted SMs in the upper and lower arms equals $N+1$, the circulating current difference tends to decrease by the amount noted in (35). Apparently, the circulating current can be controlled by adjusting the total number of inserted SMs in the upper and lower arms. However, the total number of inserted SMs is not limited to N, $N-1$, or $N+1$ but varies among $N-\lambda$, $N-\lambda+1$, $\ldots N-1, N, N+1, \ldots$, and $N+\lambda$ ($1 \leq \lambda \leq N$). Consequently, the corresponding change in the circulating current ranges from 0 to $NV_C^*T_s/2L_a$. If the value of λ is not selected correctly, the circulating current control might deteriorate along with the average SM capacitor voltage. In this study, the choice of λ followed the principle for the selection of λ in [25]. Following the analysis in [25], $\lambda = 1$ is suitable for MMC systems with lower numbers of SMs ($N < 13$), which guarantees circulating current controllability while not deteriorating the output quality. In this study, the regulation of the circulating current was implemented by selecting the total number of inserted SMs in the upper and lower arms based on the comparison between the measured circulating current and associated reference value. The reference for the circulating

current was calculated based on the real power transferred to the dc-side by

$$I_{dc}^{*} = \frac{-P}{V_{dc}}, \tag{36}$$

where $i_{circ}^{*} = I_{dc}^{*}$ for single-phase MMC system and $i_{circ}^{*} = I_{dc}^{*}/3$ for the three-phase MMC system [26]. Hence, if the measured circulating current is higher than the reference value, the total number of inserted SMs would be chosen as $N + 1$; however, $N - 1$ would be selected if the measured circulating current is lower than the reference.

From the first predefined condition corresponding to output voltage control, the difference between the numbers of inserted SMs in the upper and lower arms is acquired. Moreover, the circulating current control generates the second predefined condition for the selection of the total number of inserted SMs. From these two predefined conditions, the final value of the numbers of inserted SMs in the upper and lower arms can be calculated by simply solving a system of first-order two-variable equations using Cramer's rule:

$$N_{u\_final} = \frac{N_{sum} - N_{diff}}{2}, \tag{37}$$

$$N_{l\_final} = \frac{N_{sum} + N_{diff}}{2}. \tag{38}$$

The procedure used to calculate the number of inserted SMs in the upper and lower arms is shown in Fig. 7. It should be noted that the total number of inserted SMs for the lowest and the highest output voltage levels always equal N. For the other output voltage levels, the total numbers of inserted SMs are selected via the predefined circulating current control condition. The integer solutions of the system of first-order two-variable equations give the corresponding numbers of inserted SMs in the upper and lower arms.

C. VOLTAGE SORTING ALGORITHM

From the obtained number of inserted SMs, the voltage sorting algorithm in [27] generates the output switching signals to achieve balances SM capacitor voltages and to operate the MMC system, as shown in Fig. 8. The upper and lower arm currents are measured to identify the corresponding directions before determining the output switching states. If the arm current is positive (i.e., capacitor is charged), the SMs with the lowest capacitor voltages are inserted; similarly, the SMs with the highest capacitor voltages are inserted for the negative arm currents. Hence, the switching states are generated to operate the MMC system.

Unlike previous NLC methods, the proposed modified NLC technique indirectly calculates the numbers of inserted SMs in the upper and lower arms for the two predefined conditions for the output voltage control and circulating current control. The proposed control scheme improves the output quality of the MMC system compared to the conventional NLC and level-increased NLC methods while guaranteeing that the circulating current control and SM capacitor voltages are balanced without deteriorating the output performance.

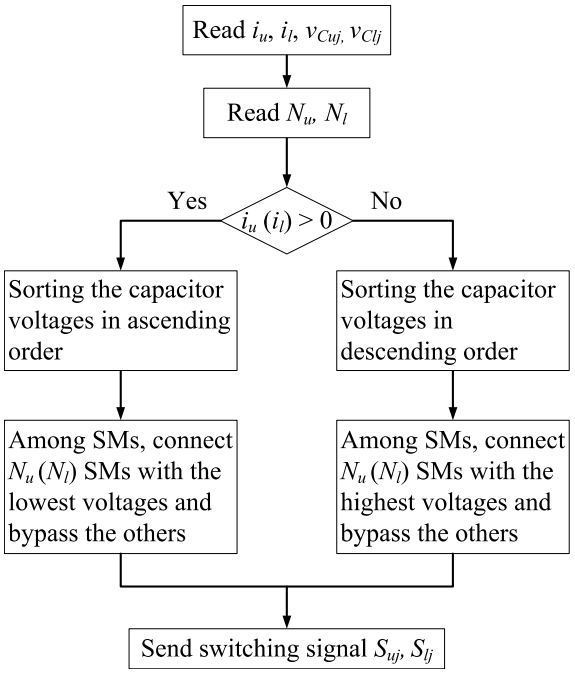

FIGURE 8. Voltage sorting algorithm.

TABLE 2. Parameters of the single-phase MMC system in the simulations and experiments.

Parameter	Simulation	Experiment
DC-link voltage V_{dc} (V)	7000	150
SMs per arm N	7	3
SM capacitor voltage V_C (V)	1000	50
SM capacitance C (mF)	2.2	2.2
Arm inductance L_a (mH)	4	3
Load inductance L (mH)	10	10
Load resistance R (Ω)	20	20
Output frequency f_o (Hz)	60	60
Rated MMC kVA S (kVA)	700	0.15
Sampling frequency f_{sp} (kHz)	10	10

V. SIMULATED AND EXPERIMENTAL RESULTS

A. SIMULATED RESULTS

Simulations were carried out in PSIM software to validate the proposed technique. The configuration of the simulated single-phase MMC is the same as that in Fig. 1(b) with 7 SMs per arm ($N = 7$). The simulation parameters are given in Table 2. To acquire comprehensive evaluations, comparisons between the proposed, modified NLC, and three previous NLC methods, including the conventional NLC, level-increased NLC II, and predictive NLC methods, were also obtained by simulation.

As shown in Fig. 9(a), the output voltage level from the conventional NLC method was eight levels ($N+1$), with the THD reaching 9.15%, whereas the THD of the output current reached 3.58%. In addition, the capacitor voltage ripple from the conventional NLC method was relatively large because of the uncontrolled circulating current. This also led to the circulating current showing a second-order harmonic

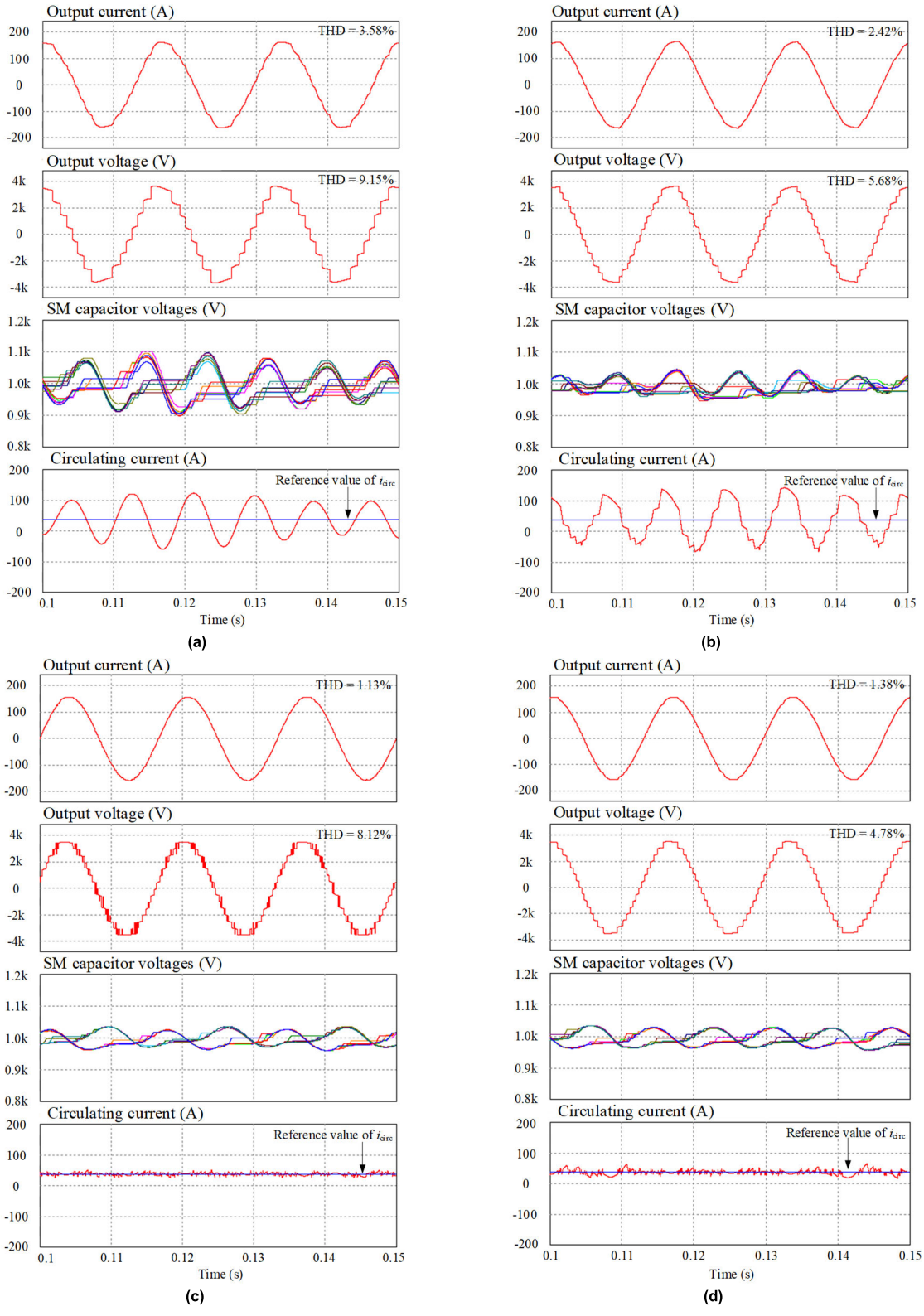

FIGURE 9. Simulated results of the (a) conventional NLC, (b) level-increased NLC II [17], (c) predictive NLC [19], and (d) proposed modified NLC.

component and high rms value (approximately 66.24 A). The level-increased NLC II method with the optimal offset, $y = 0.25$ in this simulation, increased the output voltage level by varying the total number of inserted SMs in one phase among N, $N - 1$, and $N + 1$. As a result, the output voltage level using the conventional NLC method almost doubled

from eight levels ($N+1$) to 15 levels ($2N+1$) in comparison to the level-increased NLC II method, as observed from Fig. 9(b). The step height of the output voltage was reduced from V_C^* to $0.5V_C^*$. The qualities of the output voltage and output current were improved with a lower THD of 5.68% and 2.42%, respectively, compared to the conventional NLC method. However, the variation in the total number of inserted SMs from the level-increased NLC II considerably impacted the circulating current, which reached an rms value of approximately 73.93 A.

The simulation results from the predictive NLC, as shown in Fig. 9(c), contain well-regulated output current and circulating current. The THD of the output current from the predictive NLC was low at 1.13%, whereas the rms value of the circulating current was 39 A, which is nearly the same as that of the circulating current reference value of 38.7 A. In addition, the capacitor voltages were balanced with low ripple owing to the controlled circulating current. Despite these noticeable results, the output voltage from the predictive NLC method had a substantial THD value of 8.12%. It can be noted that the total number of inserted SMs from the predictive NLC method varied with high frequency to ensure regulation of the output and circulating currents and to increase the output voltage level. This led to non-smooth transitions between the neighboring output voltage levels, as shown in Fig. 9(c). When using the proposed modified NLC method, THDs of the output current and output voltage were relatively low at 1.38% and 4.78%, respectively. As observed in Fig. 9(d), the output voltage from the proposed technique contains 15 levels and apparently smooth transitions among the adjacent levels. The capacitor voltages were well regulated at the nominal value V_C^* whereas the rms value of the circulating current (38.86 A) was close to the circulating current reference value. It can be seen from Fig. 9(d) that the peak-to-peak value of the circulating current from the proposed technique is a bit higher than in the predictive NLC method. This is attributable to the total number of inserted SMs, which was retained at N for a specific output voltage level as the lowest and the highest output voltage levels. However, the switching frequency of the proposed modified NLC method was significantly lower than that of the predictive NLC method. The comparisons between the proposed modified NLC and the three previous methods validate the operative function and merits of the proposed modified NLC method.

B. EXPERIMETAL RESULTS

The circuit diagram representing the single-phase MMC prototype is depicted in Fig. 10(a) Moreover, the photo of the prototype and control board is shown in Fig. 10(b). To verify the proposed control scheme, experiments using the proposed technique in comparison to the three previous NLC methods from the Simulations were conducted on the prototype with the parameters given in Table 2. The control circuit includes a Texas Instruments TMS320F28335 digital signal processor (DSP), voltage sensors, current sensors, etc.

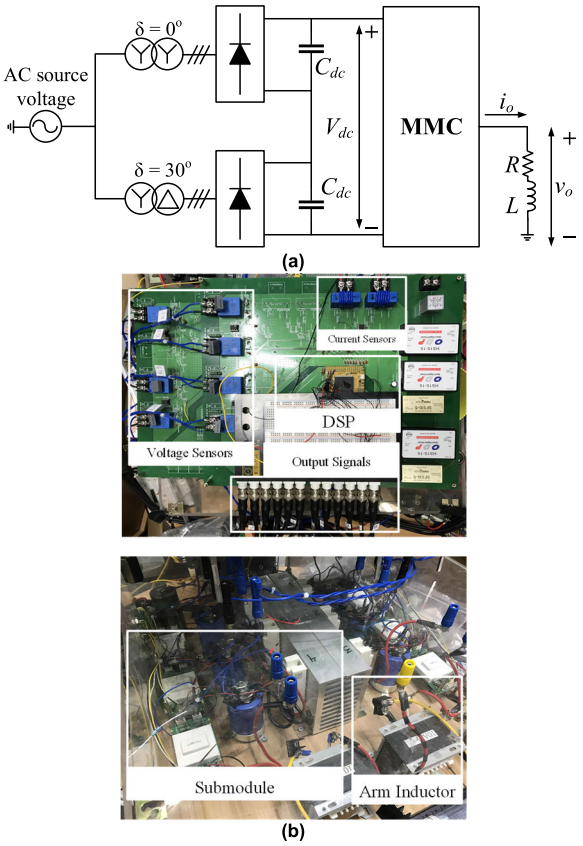

FIGURE 10. Experimental arrangement of the single-phase MMC with three SMs per arm (N = 3): (a) circuit diagram; (b) control board with the single-phase MMC prototype.

The experimental waveforms of the MMC using the conventional NLC method, level-increased NLC II method, predictive NLC, and the proposed technique are shown in Fig. 11(a)–(d), which are compatible with the simulation results. In Fig. 11(a), the output voltage from the conventional NLC contains four levels ($N+1$) with a step height of $V_C^* = 50$V. It can be found that the output current is not smoothly sinusoidal in comparison to the other NLC methods. The output current from the conventional NLC method has the highest THD value at 8.57%. The capacitor voltages are measured from the upper and lower arm SM capacitors, as illustrated in Fig. 11(a). The capacitor voltages retained balance at the nominal value of $V_C^* = 50$V, but the capacitor voltage ripple was relatively large. Meanwhile, the circulating current was dominated by the second-order harmonic component. The output voltage in Fig. 11(b) from the level-increased NLC II method had a double-level number in comparison to the conventional NLC (7 levels) with a step height of $0.5V_C^* = 25$V. The output current and capacitor voltages were better than the conventional NLC method, but the circulating current was not regulated well. In Fig. 11(c), the predictive NLC method has a seven-level ($2N+1$) output voltage and sinusoidal output current. The circulating current from the predictive NLC was minimized, similar to the results found in the Simulation section. As for

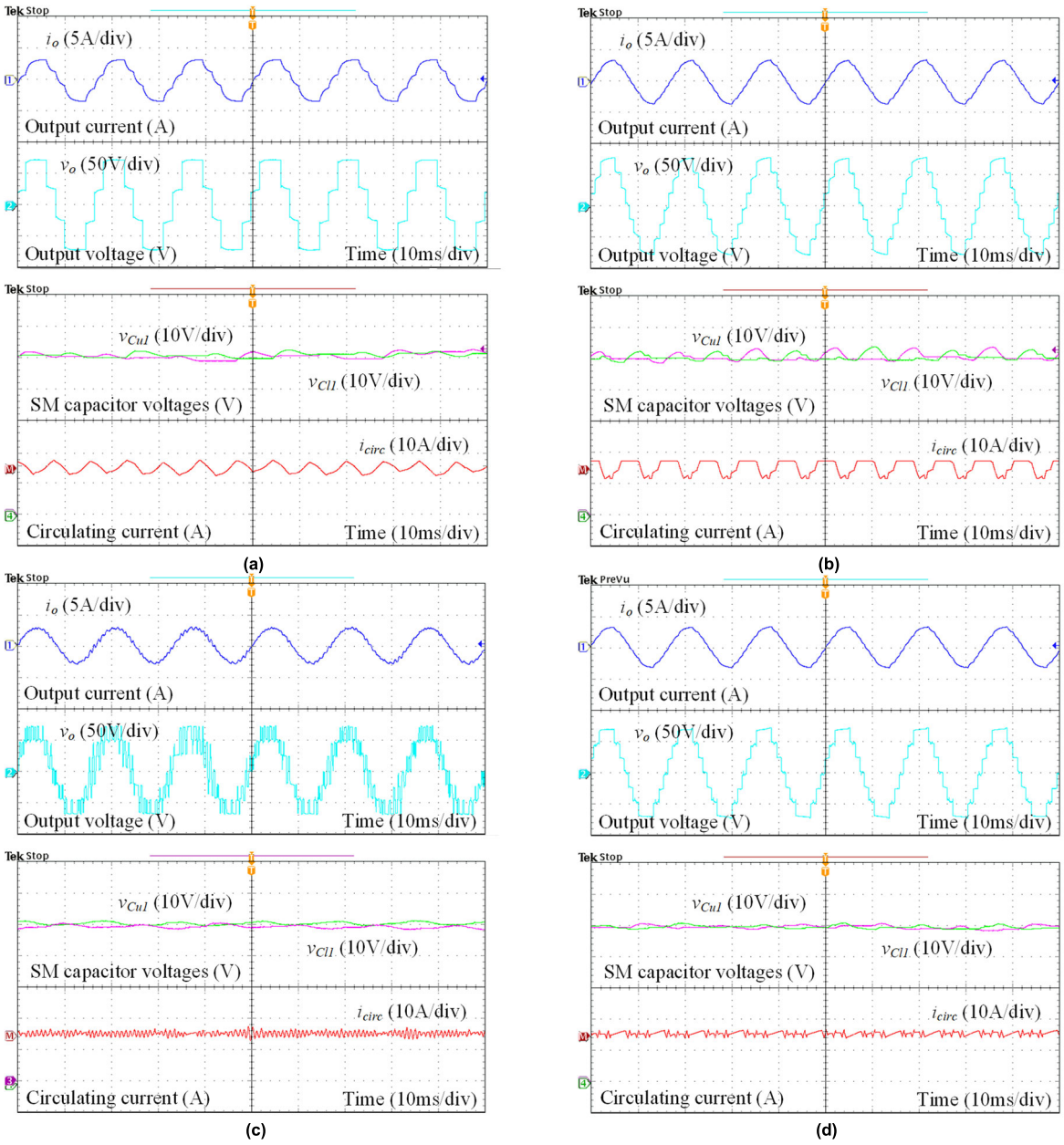

FIGURE 11. Experimental results for the (a) conventional NLC, (b) level-increased NLC II [17], (c) predictive NLC [19], and (d) proposed modified NLC.

the proposed method (Fig. 11[d]), the output voltage contained the exact seven levels as the level-increased NLC II method and the predictive NLC method, whereas the output current was a correctly sinusoidal form with a considerably low THD of 3.91%. The capacitor voltages measured from the prototype were well balanced with relatively low ripple. The circulating current was also suppressed as a result of the predictive NLC.

The THD value and frequency spectrum of the output voltage from the four methods were obtained using the power analysis application module in the Tektronix digital oscilloscope, as shown in Fig 12(a)–(d). The THD of the output voltage from the proposed technique (Fig. 12(d)) can be seen to be significantly improved compared to other NLC methods with the lowest value at 6.08%. Besides, due to the high-order harmonic components, the THD of the output voltage from the predictive NLC method (Fig. 12(c)) was notably high. The THD value of the output voltage from the level-increased NLC II method in Fig. 12(b) was improved compared to the conventional NLC method. However, due to the large magnitude of the odd-order harmonic components, it was still higher than the proposed modified NLC method. From the experimental results for the proposed technique and the other NLC methods, it can be concluded that the proposed control scheme can significantly improve the output quality of MMCs.

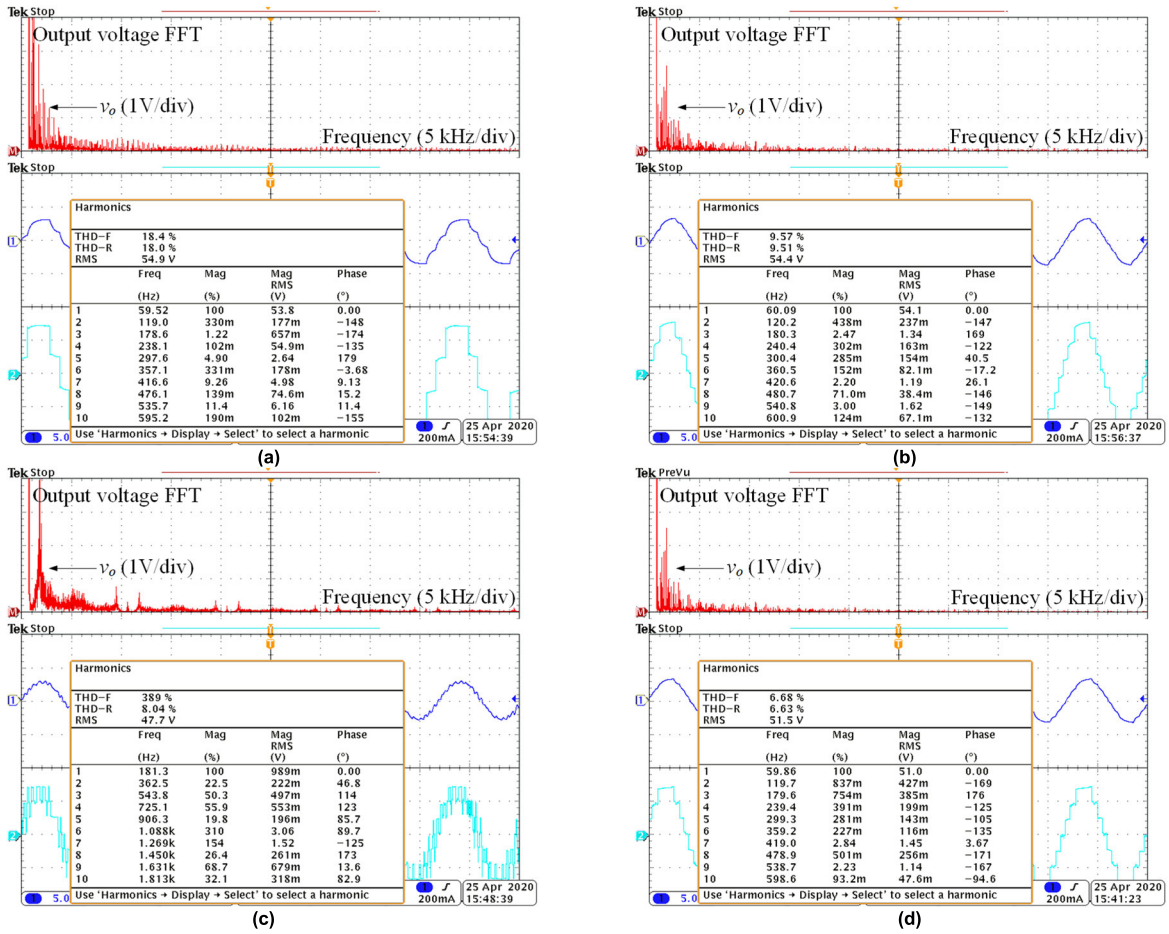

FIGURE 12. Frequency spectrum of the output voltage: (a) conventional NLC, (b) level-increased NLC II [17], (c) predictive NLC [19], and (d) proposed modified NLC.

TABLE 3. Comparison of the existing NLC methods.

Subject / Approach	Output voltage level	Circulating current control	Output current THD	Output voltage THD	Complexity
Conventional NLC [15]	$N+1$	No	High	High	Low
Level-increased NLC I [16]	$2N+1$	No	Average	Average	Low
Level-increased NLC II [17]	$2N+1$	Limited	Low	Low	Medium
NLC-C [18]	$2N-1$ to $2N+1$	Limited	Low	Low	Medium
Predictive NLC [19]	$2N+1$	Good	Low	High	High
NLC with modified circulating current suppressing strategy [20]	$2N+1$	Good	Low	High	Medium
Level-increased NLC with circulating harmonic current suppression using deadbeat control [21]	$2N+1$	Good	Low	Low	High
Proposed modified NLC	$2N+1$	Good	Low	Low	Medium

From the analysis yielded by the state-of-the-art simulations and experimental results, the comparisons among the existing NLC methods are presented in Table 3 with a description of the output voltage level, circulating current controllability, output quality, and complexity for each control scheme. The complexity depends on the additional variables needed in the controller and the programming efforts for realization. The conventional NLC method is the simplest technique to implement, but it generates a poorer output quality than others. The level-increased NLC methods improve the output quality of the MMC system. However, they do not guarantee other control objectives, such as the circulating current control or SM capacitor voltage ripple. Recent NLC methods have aimed to control the circulating

current based on previous NLC approaches, but these new methods might exert a negative impact on the output quality or be complicated. The proposed modified NLC method does not require a complicated procedure while being able to significantly improve the output quality of MMCs.

VI. CONCLUSION

This paper presented a modified NLC method to improve the output quality of MMC systems with a low number of SMs, and both the simulated and experimental studies verified the proposed technique's effectiveness. Unlike previous NLC methods for MMCs, the proposed technique guarantees the control objectives of the MMC system by defining strict conditions regarding the output voltage and circulating current controls. Moreover, the output quality is enhanced, resulting in the reduction of the output voltage and current THD, a low SM capacitor voltage ripple, and a suppressed circulating current. To ensure a comprehensive evaluation, comparisons between the proposed modified NLC and previous NLC methods have also been presented, which matched well with the design expectation.

REFERENCES

[1] S. Kouro, M. Malinowski, K. Gopakumar, J. Pou, L. G. Franquelo, B. Wu, J. Rodriguez, M. A. Pérez, and J. I. Leon, "Recent advances and industrial applications of multilevel converters," *IEEE Trans. Ind. Electron.*, vol. 57, no. 8, pp. 2553–2580, Aug. 2010.
[2] M. Malinowski, K. Gopakumar, J. Rodriguez, and M. A. Pérez, "A survey on cascaded multilevel inverters," *IEEE Trans. Ind. Electron.*, vol. 57, no. 7, pp. 2197–2206, Jul. 2010.
[3] K. Gnanasambandam, A. K. Rathore, A. Edpuganti, D. Srinivasan, and J. Rodriguez, "Current-fed multilevel converters: An overview of circuit topologies, modulation techniques, and applications," *IEEE Trans. Power Electron.*, vol. 32, no. 5, pp. 3382–3401, May 2017.
[4] J. Rodriguez, S. Bernet, P. K. Steimer, and I. E. Lizama, "A survey on Neutral-Point-Clamped inverters," *IEEE Trans. Ind. Electron.*, vol. 57, no. 7, pp. 2219–2230, Jul. 2010.
[5] H. Akagi, "Multilevel converters: Fundamental circuits and systems," *Proc. IEEE*, vol. 105, no. 11, pp. 2048–2065, Nov. 2017.
[6] A. Lesnicar and R. Marquardt, "An innovative modular multilevel converter topology suitable for a wide power range," in *Proc. IEEE Bologna Power Tech Conf.*, Jun. 2003, pp. 272–277.
[7] S. Debnath, J. Qin, B. Bahrani, M. Saeedifard, and P. Barbosa, "Operation, control, and applications of the modular multilevel converter: A review," *IEEE Trans. Power Electron.*, vol. 30, no. 1, pp. 37–53, Jan. 2015.
[8] M. Mehrasa, E. Pouresmaeil, S. Zabihi, and J. P. S. Catalao, "Dynamic model, control and stability analysis of MMC in HVDC transmission systems," *IEEE Trans. Power Del.*, vol. 32, no. 3, pp. 1471–1482, Jun. 2017.
[9] M. A. Perez, S. Bernet, J. Rodriguez, S. Kouro, and R. Lizana, "Circuit topologies, modeling, control schemes, and applications of modular multilevel converters," *IEEE Trans. Power Electron.*, vol. 30, no. 1, pp. 4–17, Jan. 2015.
[10] R. Naderi and A. Rahmati, "Phase-shifted carrier PWM technique for general cascaded inverters," *IEEE Trans. Power Electron.*, vol. 23, no. 3, pp. 1257–1269, May 2008.
[11] Y. Li, Y. Wang, and B. Q. Li, "Generalized theory of phase-shifted carrier PWM for cascaded H-Bridge converters and modular multilevel converters," *IEEE J. Emerg. Sel. Topics Power Electron.*, vol. 4, no. 2, pp. 589–605, Jun. 2016.
[12] R. Darus, J. Pou, G. Konstantinou, S. Ceballos, and V. G. Agelidis, "Circulating current control and evaluation of carrier dispositions in modular multilevel converters," in *Proc. IEEE ECCE Asia Downunder*, Jun. 2013, pp. 332–338.
[13] B. P. McGrath, C. A. Teixeira, and D. G. Holmes, "Optimized phase disposition (PD) modulation of a modular multilevel converter," *IEEE Trans. Ind. Appl.*, vol. 53, no. 5, pp. 4624–4633, Sep. 2017.
[14] S. Kouro, R. Bernal, H. Miranda, C. A. Silva, and J. Rodriguez, "High-performance torque and flux control for multilevel inverter fed induction motors," *IEEE Trans. Power Electron.*, vol. 22, no. 6, pp. 2116–2123, Nov. 2007.
[15] Q. Tu and Z. Xu, "Impact of sampling frequency on harmonic distortion for modular multilevel converter," *IEEE Trans. Power Del.*, vol. 26, no. 1, pp. 298–306, Jan. 2011.
[16] P. Hu and D. Jiang, "A level-increased nearest level modulation method for modular multilevel converters," *IEEE Trans. Power Electron.*, vol. 30, no. 4, pp. 1836–1842, Apr. 2015.
[17] L. Lin, Y. Lin, Z. He, Y. Chen, J. Hu, and W. Li, "Improved nearest-level modulation for a modular multilevel converter with a lower submodule number," *IEEE Trans. Power Electron.*, vol. 31, no. 8, pp. 5369–5377, Aug. 2016.
[18] D. Wu and L. Peng, "Characteristics of nearest level modulation method with circulating current control for modular multilevel converter," *IET Power Electron.*, vol. 9, no. 2, pp. 155–164, Feb. 2016.
[19] F. Zhang and G. Joos, "A predictive nearest level control of modular multilevel converter," in *Proc. IEEE Appl. Power Electron. Conf. Expo. (APEC)*, Mar. 2015, pp. 2846–2851.
[20] X. Chen, J. Liu, S. Ouyang, S. Song, and H. Wu, "A modified circulating current suppressing strategy for nearest level control based modular multilevel converter," in *Proc. IEEE Energy Convers. Congr. Expo. (ECCE)*, Oct. 2017, pp. 1817–1822.
[21] X. Chen, J. Liu, S. Song, and S. Ouyang, "Circulating harmonic currents suppression of level-increased NLM based modular multilevel converter with deadbeat control," *IEEE Trans. Power Electron.*, early access, Mar. 23, 2020, doi: 10.1109/TPEL.2020.2982781.
[22] K. Ilves, S. Norrga, L. Harnefors, and H.-P. Nee, "On energy storage requirements in modular multilevel converters," *IEEE Trans. Power Electron.*, vol. 29, no. 1, pp. 77–88, Jan. 2014.
[23] Z. Gong, P. Dai, X. Yuan, X. Wu, and G. Guo, "Design and experimental evaluation of fast model predictive control for modular multilevel converters," *IEEE Trans. Ind. Electron.*, vol. 63, no. 6, pp. 3845–3856, Jun. 2016.
[24] G. S. Konstantinou, M. Ciobotaru, and V. G. Agelidis, "Analysis of multicarrier PWM methods for back-to-back HVDC systems based on modular multilevel converters," in *Proc. 37th Annu. Conf. IEEE Ind. Electron. Soc. IECON*, Nov. 2011, pp. 4391–4396.
[25] B. Gutierrez and S.-S. Kwak, "Modular multilevel converters (MMCs) controlled by model predictive control with reduced calculation burden," *IEEE Trans. Power Electron.*, vol. 33, no. 11, pp. 9176–9187, Nov. 2018.
[26] M. Vatani, B. Bahrani, M. Saeedifard, and M. Hovd, "Indirect finite control set model predictive control of modular multilevel converters," *IEEE Trans. Smart Grid*, vol. 6, no. 3, pp. 1520–1529, May 2015.
[27] S. Rohner, S. Bernet, M. Hiller, and R. Sommer, "Modulation, losses, and semiconductor requirements of modular multilevel converters," *IEEE Trans. Ind. Electron.*, vol. 57, no. 8, pp. 2633–2642, Aug. 2010.

MINH HOANG NGUYEN received the B.S. degree in electrical and electronics engineering from the Hanoi University of Science and Technology, Vietnam, in 2016. He is currently pursuing the combined M.S. and Ph.D. degree in electrical and electronics engineering with Chung-Ang University, Seoul, South Korea. His research interest includes a control for multilevel converters.

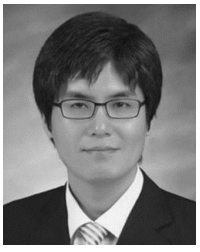

SANGSHIN KWAK (Member, IEEE) received the Ph.D. degree in electrical engineering from Texas A&M University, College Station, TX, USA, in 2005. From 2007 to 2010, he was an Assistant Professor with Daegu University, Gyeongsan, South Korea. Since 2010, he has been with Chung-Ang University, Seoul, South Korea, where he is currently a Professor. His research interests include topology design, and the modeling, control, and analysis of ac/dc, dc/ac, and ac/ac power converters, including resonant converters for adjustable-speed drives and digital display drivers, as well as modern control theory applied to digital-signal-processing-based power electronics.